SEPARATING THE LIVING FROM THE DEAD: AN ELECTROPHORETIC APPROACH

Viswateja Kasarabada[†], Nuzhet Nihaar Nasir Ahamed[†], Alaleh Vaghef-Koodehi[†], Gabriela Martinez-Martinez[†], and Blanca H. Lapizco-Encinas[†, *]

[†] Microscale Bioseparations Laboratory and Biomedical Engineering Department, Rochester Institute of Technology, 160 Lomb Memorial Drive, Rochester, New York, 14623, United States.

*Email: bhlbme@rit.edu

Keywords:

Cell viability

Electrokinetics

Microfluidics

Nonlinear electrophoresis

Separation of cells

ABSTRACT

Cell viability studies are essential in numerous applications, including drug development, clinical analysis, bioanalytical assessments, food safety and environmental monitoring. Microfluidic electrokinetic (EK) devices have been proven to be effective platforms to discriminate microorganisms by their viability status. Two decades ago, live and dead *Escherichia coli* (*E. coli*) cells were trapped at distinct locations in an insulator-based EK (iEK) device with cylindrical insulating posts. At that time, the discrimination between live and dead cells was attributed to dielectrophoretic effects. This study presents the continuous separation between live and dead *E. coli* cells which was achieved primarily by combining linear and nonlinear electrophoretic effects in an iEK device. First, live and dead *E. coli* cells were characterized in terms of their electrophoretic migration, then, the properties of both live and dead *E. coli* cells were input into a mathematical model built using COMSOL *Multiphysics*® software to identify appropriate voltages for performing an iEK separation in a T-cross iEK channel. Subsequently, live and dead cells were successfully separated experimentally in the form of an electropherogram achieving a separation resolution of 1.87. This study demonstrated that linear and nonlinear electrophoresis phenomena are responsible for the discrimination between live and dead cells under DC electric fields in iEK devices. Continuous electrophoretic assessments, such as the one presented here, can be used to discriminate between distinct types of microorganisms, including live and dead cell assessments.

INTRODUCTION

Cell viability analyses are essential in many fields such as new drug development, clinical analysis, bioanalytical assessments, and food safety and environmental monitoring.[1] A major driver for the development of new cell viability assessment methods is the rise of antibiotic-resistant bacteria, a major cause of concern with the significant increase in nosocomial infections. An estimated number of 687,000 infections and 72,000 deaths occurred in 2019, according to the US Center for Disease Control, placing the cost to the healthcare at over 25 billion dollars.[1,2]

Microfluidic devices are an attractive option for cell assessments as they offer rapid response times and portability.[3–5] Electrokinetics (EK), one of the major branches of microfluidics, has received significant attention as it offers label free and robust characterization methods that depend on the physical characteristics of the microorganisms rather than requiring a labeling agent. Several review articles have highlighted the potential of microscale EK devices for the effective separation, sorting and analysis of a wide range of microparticles and cells,[6–8] including a detailed article by Patel and Markx[9] on EK techniques for assessing cell viability.

There are a plethora of EK-based devices developed for the discrimination between live and dead microorganisms.[10–18] Dielectrophoretic effects have been reported to be the discriminatory mechanism, where live cells exhibit positive DEP (pDEP) and are attracted to the regions of higher electric field gradient, while dead cells migrate away from these regions under the effects of negative DEP (nDEP). The first reported EK differentiation between live and dead cells was done by Pohl and Hawk[10] in 1966 with the DEP-based separation of live and dead *Saccharomyces cerevisiae* (*S. cerevisiae*) cells. They employed a rudimentary electrode-based system stimulated with AC potentials featuring with two orthogonally placed pin and plate electrodes in a cylindrical chamber. Live cells were observed to gather quickly at the pin electrode under pDEP effects, while dead cells remained behind showing no response. Li and Bashir[14] in 2002 utilized DEP to differentiate between live and dead *Listeria innocua* cells employing an array of interdigitated electrodes stimulated by AC potentials. In their device, live cells exhibited pDEP while dead cells exhibited nDEP. In 2004, Lapizco-Encinas *et al.*[11] discriminated between live and dead *Escherichia coli* (*E. coli*) cells in an DC stimulated insulator-based EK (iEK) device by trapping them at different

locations within an array of cylindrical insulating posts. In 2010, Iliescu *et al.*,[16] designed an AC stimulated 3D electrode-based system to trap live and dead *S. cerevisiae* cells with pDEP and nDEP, while in 2015 Zellner *et al.*,[19] utilized an iEK device with DC-biased AC fields to selectively trap live *Staphylococcus aureus* cells from a sample containing live and dead cells. More recently, in 2020 and 2021 Ettehad *et al.*,[20,21] separated live and dead *S. cerevisiae* cells employing AC potentials in a device with interdigitated electrodes, where live cells were selectively trapped with pDEP, while dead cells were flushed away. Electrokinetic devices have also been employed to inactivate cells as reported by Pudasaini *et al.* with the inactivation of *Enterococcus faecalis*, *E. coli*, and *S. cerevisiae* cells by means of electroporation employing iEK devices with insulating pillars[22,23] and insulating microbeads.[24] The cells were inactivated by exposure to high electric fields (up to 18.5 kV/cm) that irreversibly ruptured the cell membrane. Ho *et al*., combined deterministic lateral displacement with EK to separate live and dead cells *E. coli* and *S. cerevisiae* strains, employing microdevices with large post arrays and two distinct outlets; collecting separated fractions of live and dead cells with purity above 90%.[25]

Recently the field of iEK experienced a major change, since it was identified that nonlinear electrophoresis (EP_{NL}) effects can be a major force influencing the migration of particles and microorganisms under high electric magnitudes in systems stimulated by DC and DC-biased low frequency AC potentials. The reports by Rouhi and Diez,[26] Tottori *et al.*,[27] and Cardenas-Benitez *et al.*,[28] revealed experimentally the strong effect of EP_{NL} on the migration of polystyrene microparticles in iEK systems stimulated by DC potentials. Follow-up work has demonstrated that microorganisms are equally affected by EP_{NL} forces.[29–31] The first studies on EP_{NL} were reported in early 1970s by Dukhin and colloborators.[32] Further developments[33,34] have advanced the knowledge on EP_{NL}, however, the lack of experimental data hindered the wide-spread application of EP_{NL} in analytical separations.[35] The recent reports on the characterization of the mobility of EP_{NL} of polystyrene microparticles, cells and viruses[28,31,36–39] have enabled highly discriminatory separations.[29,30,40,41]

The discrimination between live and dead cells in an iEK system employing DC potentials was first reported in 2004 by Lapizco-Encinas *et al.*[11] At that time it was assumed that the live/dead discrimination was due to DEP effects, where dead cells were thought to have a lower magnitude of nDEP effects compared to live cells that also exhibited a nDEP behavior. The recent reports on the effects of EP_{NL} on particle and cell migration give insight that DEP effects may not have been responsible for the reported live and dead cell discrimination under DC potentials.[11] While it is well-accepted that DEP is the dominant effect in EK systems stimulated with AC potentials, this report presents a different interpretation of the results observed in EK systems stimulated with DC and DC-biased low frequency AC potentials.

This report is focused on discerning the EK mechanisms responsible for the discrimination between live and dead *E. coli* cells in an iEK microchannel with cylindrical insulating posts under DC potentials, by employing mathematical modeling with COMSOL *Multiphysics*® and experimentation. First, live and dead cells were characterized in terms of their electromigration velocity employing particle tracking velocimetry (PTV) in a rectangular microchannel (**Fig. 1a**). This allowed for the determination of their electrophoretic mobilities, both linear and nonlinear regimes. The characterization data was then employed as the input to a COMSOL model to identify the conditions and predict the retention times ($t_{R,p}$) for a successful separation between the live and dead cells. Experimental separations between the live and dead cells were performed employing a T-cross iEK channel (**Fig. 2**), obtaining electropherograms from which experimental retention times ($t_{R,e}$) were assessed. A separation resolution (Rs) of 1.87 was achieved, demonstrating that live and dead cells differ enough in their electrophoretic migration, to allow for a successful separation. Good reproducibility in terms of retention times was obtained between experimental repetitions, with deviations below 11% for live and dead cells. Good agreement between the modeling and experimental results was obtained with deviations between $t_{R,p}$ and the average $t_{R,e}$ below 18% in

all cases. The findings from this work illustrate that electrophoretic effects, both linear and nonlinear, can be employed in iEK systems under DC potentials to effectively discriminate between distinct types of cells, including live and dead assessments.

THEORY

Electrokinetic phenomena are classified as linear and nonlinear, as determined by their dependance on the electric field magnitude. The overall velocity ($\mathbf{v}_P$) of a particle in an iEK microfluidic channel is described as a summation of the following linear and nonlinear EK effects:

$$\mathbf{v}_P = \mathbf{v}_{EO} + \mathbf{v}_{EP,L} + \mathbf{v}_{EP,NL}^{(n)} + \mathbf{v}_{DEP} \quad (1)$$

where $\mathbf{v}_{EO}$ is the electroosmotic (EO) velocity, $\mathbf{v}_{EP,L}$ is the linear electrophoretic (EP_L) velocity, $\mathbf{v}_{EP,NL}^{(n)}$ is the nonlinear electrophoretic (EP_{NL}) velocity, where n represents the nonlinear dependence with the magnitude of electric field ($\mathbf{E}$), and $\mathbf{v}_{DEP}$ is the dielectrophoretic (DEP) velocity. Cardenas-Benitez *et al.*,[28] identified the condition of electrokinetic equilibrium condition (E_{EEC}) under which $\mathbf{v}_P$ becomes zero inside a rectangular microchannel (**Fig. 1b**).

The velocity expressions of the two linear EK mechanisms considered here are:

$$\mathbf{v}_{EO} = \mu_{E0}\mathbf{E} = -\frac{\varepsilon_m \zeta_W}{\eta}\mathbf{E} \quad (2)$$

$$\mathbf{v}_{EP,L} = \mu_{EP,L}\mathbf{E} = \frac{\varepsilon_m \zeta_P}{\eta}\mathbf{E} \qquad \text{(weak field regime)} \quad (3)$$

where μ_{E0} and $\mu_{EP,L}$ are the mobilities of EO flow and EP_L, respectively; ε_m and η are the permittivity and viscosity of the suspending medium, respectively; and ζ is the zeta potential at the interface between the suspending medium and the channel wall or the particle. **Equations (2-3)** are based on Smolchowski's approximation which is valid under conditions of a thin electrical double later (EDL) which is fulfilled in the current study. **Equation (2)** is a common simplification obtained employing the Helmholtz-Smoluchowski approximation which describes EO flow velocity outside of the EDL.[42] **Equation (3)** assumes that the particle migrates with a constant electrophoretic velocity as the driving force exerted by the electric field on the particle and the electrical double layer (EDL) is balanced by the hydrodynamic drag for exerted on the particle and the ions, resulting a net zero force.[43,44] This force balance is valid in the absence of pressure driven flow, which is a condition fulfilled in this study.

The two nonlinear EK phenomena considered here are EP_{NL} and DEP. To identify the regime of EP_{NL} three dimensionless parameters are utilized: the dimensionless applied field magnitude (β), the Peclet number (Pe) and the Dukhin number (Du). The expressions employed are described below:

$$\beta = \frac{E\, r_p}{\varphi} \quad (4)$$

$$Pe = \frac{r_p |\mathbf{v}_{EP}|}{D} \quad (5)$$

$$Du = \frac{K^\sigma}{K^m r_p} \quad (6)$$

where r_p is the particle radius, φ is the thermal voltage (~25 mV), $|\mathbf{v}_{EP}|$ is the magnitude of the electrophoretic velocity (linear and nonlinear contributions), D is the diffusion coefficient, and K^σ and K^m are the surface conductivity and bulk conductivity of the medium, respectively. There are two well-defined analytical models that

describe the velocity of EP_{NL} for the two limiting cases of low and high *Pe* number (no models are available yet for intermediate Pe values).[45]

$$\mathbf{v}_{EP,NL}^{(3)} = \mu_{EP,NL}^{(3)} E^3 \widehat{\boldsymbol{a}_E} \qquad \text{for } \beta \leq 1,\ Pe << 1,\ Du \text{ arbitrary (moderate field regime)} \qquad (7)$$

$$\mathbf{v}_{EP,NL}^{(3/2)} = \mu_{EP,NL}^{(3/2)} E^{3/2} \widehat{\boldsymbol{a}_E} \qquad \text{for } \beta > 1,\ Pe >> 1,\ Du << 1 \text{ (strong field regime)} \qquad (8)$$

where $\mu_{EP,NL}^{(n)}$ is the mobility of EP_{NL} and $\widehat{\boldsymbol{a}_E}$ is the unit vector for the electric field. In this study, only the moderate ($\sim E^3$) regime of EP_{NL} was considered since experimental conditions did not allow for the strong field regime to be reached as the maximum values of β and Pe were as follows: $\beta_{max} =$ 0.7 and $Pe_{max} = 0.19$. The values of the dimensionless parameters used to identify the regimes of EP_L and EP_{NL} are included in **Tables S1** and **S2**.

The expression of the DEP velocity for a spherical particle is defined as:

$$\mathbf{v}_{DEP} = \mu_{DEP} \nabla E^2 = \frac{r_p^2 \varepsilon_m}{3} \mathrm{Re}[f_{CM}] \nabla E^2 \qquad \text{where} \quad f_{CM} = \left[\frac{\sigma_p - \sigma_m}{\sigma_p + 2\sigma_m}\right] \text{under DC fields} \qquad (9)$$

where μ_{DEP} is the DEP mobility, ∇E^2 is the gradient of the square of electric field magnitude, f_{CM} is the Clausius-Mossotti factor which defines particle polarizability, which under DC conditions is estimated employing the conductivity of the particles (σ_p) and the medium (σ_m). Estimations of the DEP velocity employed the expression for a prolate shaped particle included in the supplementary material. Under DC conditions the electric field only penetrates the cell membrane, thus, the values of cell membrane conductivities were considered when estimating the f_{CM}. The values of the membrane conductivities of the live and dead cells were obtained from the literature and are listed in **Table 1**.

The quality of the separations was determined by estimating the separation resolution (Rs) between the peaks in the electropherogram, which was calculated as follows:

$$Rs = \frac{1.18\,(t_{R2,e} - t_{R1,e})}{W_1 + W_2} \qquad (10)$$

where $t_{R,e}$ is the experimental retention time of the cells in the post array of the iEK microchannel (**Fig. 2**) and W is the width of the peak measured at half of the peak's height.

EXPERIMENTAL SECTION

Cell Samples. This study employed *E. coli* cells (ATCC 11775, American Type Culture Collection, Manassas, VA, USA) as listed in **Table 1**. Standard cell culture techniques were followed to obtain the live *E. coli* cells. To prepare the sample of dead cells, a sample of live cells was taken and placed in a water bath at 80 ºC for 20 minutes, rendering the cells non-viable. Both live and dead cell samples at concentration of 7 x10^8 cells/ml were stained with a combination of propidium iodide (PI) and SYTO 9 fluorescent dyes (ThermoFisher, Carlsbad, CA, USA).[46] SYTO 9 stain is able to penetrate live and dead cells, while PI stain penetrates only dead cells due to their compromised membrane. Live cells fluoresced in green color as they only contained the SYTO 9 stain, while dead cells contained both dyes, but fluoresced in red color as PI dominates over SYTO 9 when both the dyes are present.

Microdevices. All devices were fabricated employing standard soft lithography techniques[47] utilizing molds made with SU8 on a silicone wafer. All microchannels were cast employing polydimethylsiloxane (PDMS – Dow Corning, MI, USA), to create a rectangular microfluidic channel employed for PTV illustrated in **Figure 1a** and a T-cross iEK channel employed for separation experiments in **Figure 2**.

Suspending Medium. A buffer solution of K_2HPO_4 at a concentration of 0.2 mM was employed as the suspending medium for all experiments, this produces an electrical double layer with a thickness of 14 nm. Tween 20 was added at 0.05% (v/v) to decrease cells from sticking to the channel walls. This media had a pH of 7.2 ± 0.2, and a conductivity of 44.1 ± 1.7 µS/cm. For this suspending medium, in the PDMS devices used in this work, it resulted in a wall zeta potential, ζ_W of -60.1 ± 3.7 mV and μ_{EO} of 4.7 ± 0.3 $\times 10^{-8}$ $m^2V^{-1}s^{-1}$, as assessed with current monitoring.[48]

Equipment and Software. A Leica DMi8 inverted microscope (Wetzlar, Germany) was employed to record the characterization experiments, while the separation experiments were recorded as videos using a Zeiss Axiovert 40CFL inverted microscope (Carl Zeiss Microscopy, Thornwood, NY, USA). Voltage sequences were applied to the devices with four platinum wire electrodes (1.5 cm length and 0.6 mm diameter) labelled A – D (**Fig. 2**) employing a high voltage power supply (Model HVS6000D, LabSmith, Livermore, CA, USA). Tracker© software (Douglas Brown) built on Open Source Physics (OSP)[49] Java framework was used to analyze the particle positions for characterization videos and ImageJ was used to analyze the pixel density of *E. coli* cells to track the fluorescence signals for separation experiments.

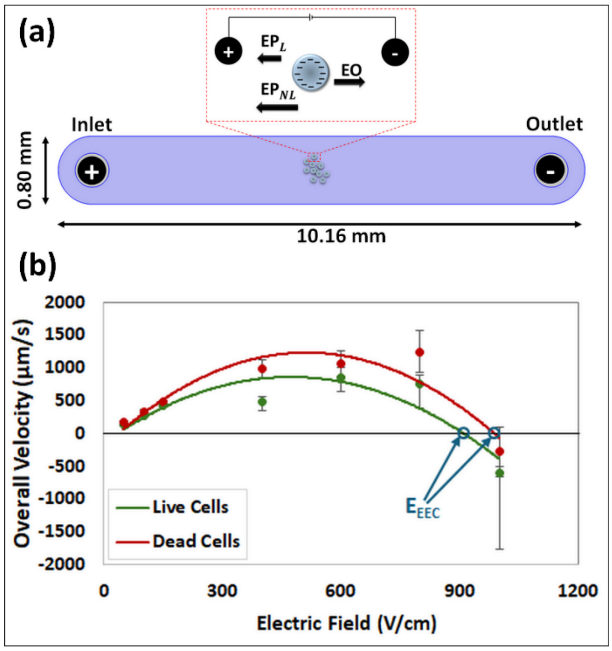

Figure 1. (a) Illustration of the rectangular microfluidic channel utilized in the PTV characterization of live and dead cells with an inset showing the forces exerted on the cells (no DEP effects are present). **(b)** Plot of the overall cell velocity as a function of electric field, depicting the E_{EEC} for both live and dead cells. As observed, live cells cross the zero-velocity line at a lower electric field magnitude than dead cells.

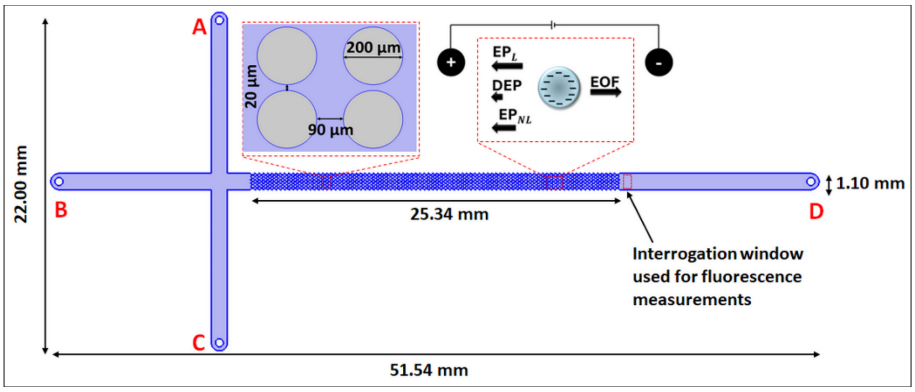

Figure 2. Illustration of the T-cross iEK channel employed for the separation between live and dead cells, depicting the channel dimensions and the interrogation window used to acquire the fluorescence measurements used to build the electropherogram in **Figure 3**. The first inset illustrates the dimensions of the insulating posts, and the second inset illustrates the EK forces exerted on the cells.

COMSOL Model. Mathematical modeling has proven to be a valuable tool to guide EK experimentation and device design.[29,50,51] A COMSOL *Multiphysics* model was built to identify appropriate voltage conditions and predict the retention times ($t_{R,p}$) of the cells in the insulated post array of the iEK channel shown in **Figure 2**. These values were predicted by inputting into COMSOL the EK characteristics of the live cells and dead cells obtained with PTV experiments.[36–38] COMSOL simulations were performed to identify a set of applied voltages that would result in a difference of predicted retention times of 20 s ($\Delta t_{R,p}$ ~ 20 s). Detailed model information is included in the supplementary material **(Figures S1-S2** and **Tables S3-S4).** The cutline shown in **Figure S2** was used to obtain the velocity data employed to estimate $t_{R,p}$ values under a range of voltages, these results are included in the supplementary material (**Table S5**).

Experimental Procedure. Experiments were conducted in two stages – characterization and separation. Prior to experimentation, all devices were soaked for 12 h in the suspending medium to ensure stable EO flow. Prior to each experiment pressure driven flow was eliminated by balancing the liquid levels at the inlet and outlet reservoirs. A set of PTV assessments were conducted in the device shown in **Figure 1a** to characterize the migration velocity (**Fig. 1b**) of the cells and obtain the cell dielectric properties listed in **Table 1**. This information was then employed for mathematical modeling which guided experimentation. Separation experiments were conducted employing the T-cross iEK channel shown in **Figure 2**. After the iEK channel was filled with the suspending, platinum electrodes were placed in all four liquid reservoirs. Then, a 10 µL sample of the live and dead cells at a concentration of 7 x10^8 cells/ml was introduced at reservoir A (**Fig. 2**). A three-step EK injection process was utilized to electrokinetically introduce the sample into the main channel, the voltages and time durations of EK injection process are listed in **Table 2**. The elution of the cells from the post array was recorded at the interrogation window marked in **Figure 2**. The recorded videos were analyzed using the ImageJ software to assess the fluorescence signal of the live and dead cells. A snippet of the image analysis method is included in **Figure S3**. The separation experiment was repeated three times to ensure reproducibility, the reproducibility results are in **Table S6**.

RESULTS AND DISCUSSION

Characterization of the Dielectric Properties of Cells. Live and dead cells were characterized in the PTV channel illustrated in **Figure 1a**. The Information on cell size and EK properties is listed in **Table 1**. The overall cell velocity was obtained from PTV experiments and plotted as a function of the electric field as shown in **Figure 1b**. Both cells in this study had a negative surface charge, as demonstrated by their negative zeta potential values which only differed by 7 mV. A negative surface charge means that their electrophoretic migration is towards the inlet, opposite to the direction of EO flow. The E_{EEC} of the live and dead cells (**Fig. 1b**) was as expected, with live cells crossing the zero-velocity line at lower electric field than dead cells. Live cells possess a higher magnitude in their electrophoretic mobilities (linear and nonlinear), resulting in live cells exhibiting a stronger electrophoretic pull towards the inlet, which decreases their $\mathbf{v}_P$ magnitude, i.e., live cells migrate at a lower speed. The $\mathbf{v}_P$ values measured in the channel in **Figure 1a** follow **Equation 1**, minus DEP effects, as the electric field in this channel is homogenous, no DEP effects are present, since DEP requires an electric field gradient. Size measurements of the *E. coli* cells showed a slight difference between live and dead cells. These results of negligible size differences between live and dead *E. coli* cells are in agreement with the studies by Bao *et al*. [25] and Kłodzińska *et al*.[52]

Table 1. Characteristics of the live and dead cells used in this study.

Cells	Dimensions (μm)	ζ_P (mV)	$\mu_{EP,L}$ x10^{-8} (m^{2}V^{-1}s^{-1})	$\mu^{(3)}_{EP,NL}$x10^{-18} (m^{4}V^{-3}s^{-1})	E_{EEC} (V/cm)	σ_p (μS/cm)
E. coli (Live)	Length: 3.2 ± 0.3 Width: 1.1 ± 0.2	-25.5 ± 1.5	-2.0 ± 0.1	-6.4 ± 0.6	911.6 ± 3.3	0.01[53]
E. coli (Dead)	Length: 3.4 ± 0.6 Width: 1.0 ± 0.3	-18.5 ± 0.8	-1.4 ± 0.1	-4.9 ± 0.6	963.1 ± 9.8	100[53,54]

Continuous Separation Between Live and Dead Cells. Continuous separation experiments were conducted in the T-cross iEK channel with cylindrical posts shown in **Figure 2**. There are two types of separations performed in iEK channels: continuous separations which employ the streaming EK regime,[29] and trapping separations which enrich and separate particles using the EK trapping regime.[55] The streaming regime is when particles inside the iEK channel flow in streamlines under the effects of linear and nonlinear EK phenomena. The trapping EK regime is when nonlinear EK phenomena (EP_{NL} in this case) are strong enough to overcome EO flow and particles are "trapped" at specific locations within the channel.[56] The present study separated live and dead *E. coli* cells employing the streaming EK continuous approach and compare these results with the trapping EK approach used in first live dead cell discrimination study in an iEK channel reported in 2004.[11] A device with cylindrical insulating posts (**Fig. 2**) was employed for the separation experiments in this study with the purpose of achieving the closest possible comparative analysis with the 2004 report. **Figure 3a** illustrates the results reported by Lapizco-Encinas *et al.* in 2004.[11] In that study, a mixture of live and dead *E. coli* cells was introduced into a simple iEK channel with cylindrical posts (200 μm diameter, spaced 250 μm center-to-center), and after applying a DC voltage of 720 V over the 10.2 cm long channel (E overall = 600 V/cm), both live and dead cells were electrokinetically trapped. As shown in **Figure 3a**, dead cells (red) were trapped as a band located closer to the constriction between the insulating posts, while live cells (green) were trapped in a band located farther from the constriction, behind the band of dead cells. This was the first report on differential iEK trapping of live and dead cells. At that time, the distinct behavior exhibited by the live and dead cells was attributed to DEP effects caused by significant differences in the membrane conductivity of the cells. They considered that live cells had a membrane conductivity of 1 x10^{-4} μS/cm[57] while the dead cells had an increase by a factor of 10^4 in their membrane conductivity,[54] making the dead cell membrane conductivity to be ~1 μS/cm. Considering that the suspending media employed had a conductivity of 22.5 μS/cm,

the study from 2004 reported that both cells exhibited nDEP behavior. In the discussion of the results of the 2004 report,[11] it was stated that live *E. coli* cells exhibited a greater magnitude of the nDEP behavior than dead cells due their lower membrane conductivity which in turn produced a higher magnitude of their negative Clausius-Mossotti factor (f_{CM}). Similar results were reported by Gallo-Villanueva *et al*., with the trapping of live and dead *Selenastrum capricornutum* microalgae cells.[58] This interpretation of the results based on DEP was well accepted for decades. However, the recent work on EP_{NL} in iEK systems,[26–28,36–38] also demonstrated that the relative magnitude of DEP effects is actually low, since $\mathbf{v}_{DEP}$ is less than 6% of the overall magnitude of $\mathbf{v}_{EP,NL}^{(3)}$,[46] i.e., DEP effects are not dominant and cannot cause particle/cell trapping in systems stimulated with DC fields or low frequency AC fields. Instead, the distinct locations of the bands of trapped live and dead cells can be explained in terms of electrophoretic effects. Live cells, which have greater magnitudes of their negative electrophoretic mobilities than dead cells (**Table 1**), experience a greater electrophoretic pull towards the inlet, thus, resulting in a trapping/band location ($\mathbf{v}_P = 0$) in a region of lower electric field magnitude than that of dead cells.

The present studied the continuous separation between live and dead *E. coli* cells employing the new knowledge on EP_{NL}.[26–28,36–38] After live and dead cells were characterized in terms of their ζ_P, $\mu_{EP,L}$ and $\mu_{EP,NL}^{(3)}$ values, COMSOL modeling results that indicated a difference in retention times of approximately 20 s could be obtained with voltages applied at reservoirs A, B, C, D (as shown in **Fig. 2**) being 200 V, 800 V, 200 V and 0 V, respectively. A summary of the complete modeling results is included in **Table S5**. The voltages sequence employed for the iEK injection process are listed in **Table 2**. The experimental results showed, as expected, live cells to have a lower overall velocity ($\mathbf{v}_P$) than dead cells, as seen in **Figures 3b-3d**. Dead cells (red) are migrating ahead of live cells (green). The electropherogram in **Figure 3e** illustrates the successful separation between live and dead *E. coli* cells, with a *Rs* = 1.87. A video of the separation, depicting the elution of the cells is included in the supplementary material (**Video S1**).

Table 2. Voltages employed for EK sample injection and the iEK separations of live and dead cells.

Description	Step	Runtime (s)	Applied voltage (V) at each reservoir			
			A	B	C	D
Separation of live and dead *E. coli*	Loading	8	1500	500	0	1000
	Gating	2	1000	1000	800	0
	Injection	350	200	800	200	0

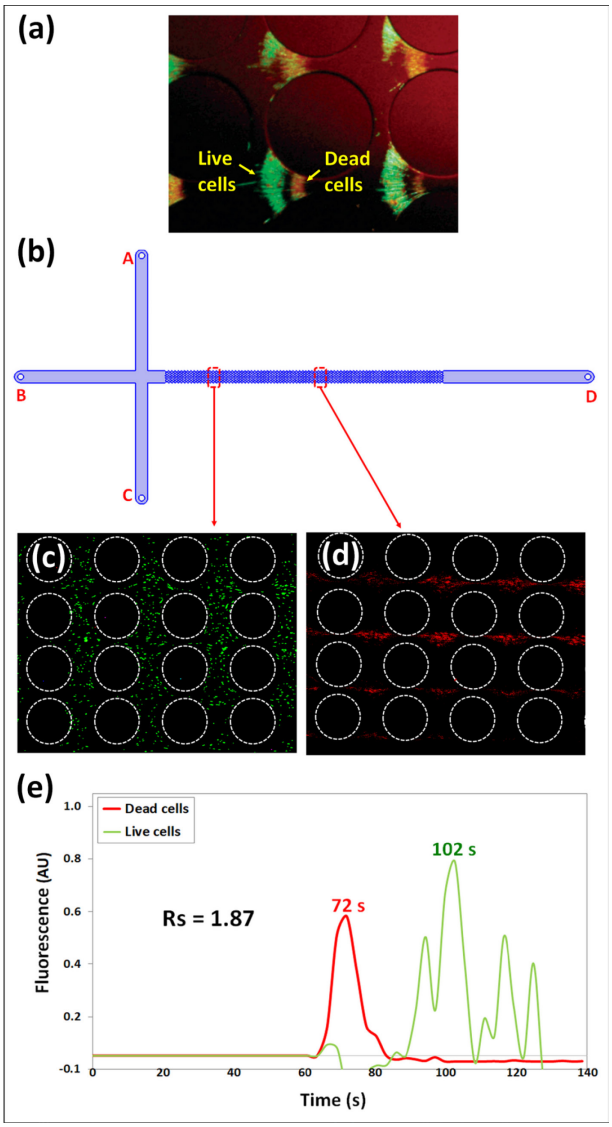

Figure 3. (a) Differential trapping of live (green) and dead (red) *E. coli* cells at the constriction regions between the cylindrical insulating posts at potential of 720 V applied over a 10.2 mm long channel (E overall = 600 V/cm). Adapted with permission from Ref.,[11] copyright (2004) American Chemical Society (ACS). **(b)** Illustration of the iEK microchannel showing two distinct locations for observation of the migrating cells. **(c)** Live *E. coli* cells migrating closer to the start of the post array. **(d)** Dead *E. coli* cells migrating ahead of the live cell at a location close the center of the post array. The two images of the migrating cells were taken at time = 55 s after the EK injection. **(e)** Electropherogram of the live and dead *E. coli* cells separation built by employing the fluorescence signal obtained at the interrogation window indicated in **Figure 2**. A resolution of Rs = 1.87 was obtained with the following applied voltages: V_A = 200 V, V_B = 800 V, V_C = 200 V and V_D = 0 V, resulting E overall = 137.4 V/cm.

The results in **Figure 3e** show that dead cells eluted before live cells, at 72 s vs. 102 s, which is as expected from the PTV results in **Figure 1b** and the electrophoretic mobility values in **Table 1**. There was a small number of live cells that eluted with the dead cells indicating some of the live cells had died after the labelling process causing them to elute with the dead cells. The live cells elute in three distinct peaks, perhaps due to a greater population distribution than dead cells. The experiment ended 150 s after the cells entered the post array taking the total experiment duration to approximately 3 minutes. The short duration of the experiment shows the potential of

utilizing iEK separation as a rapid cell viability assessment. **Table 3** summarizes the retention times results from the electropherogram in **Figure 3e** and compares the experimental values to the COMSOL predicted retention time values. The deviations between $t_{R,e}$ and $t_{R,p}$ values were 9% and 26% for live and dead cells, respectively, indicating a fair agreement between the model and the experiments. Good experimental reproducibility was obtained between experimental repetitions, with deviations below 11% in terms of $t_{R,e}$ values (**Table S6**). When comparing $t_{R,p}$ values to the average from all experimental repetitions, $\overline{t_{R,e}}$, it was found that the deviations between model and experiments were below 18% (**Table S7**).

Table 3. Results from the separation between live and dead cells from the electropherogram shown in **Figure 3e**.

Cell	Rs	COMSOL predicted $t_{R,p}$ (s)	Experimental $t_{R,e}$ (s)	Deviation $t_{R,p}$ vs. $t_{R,e}$ (%)
E. coli (Live)	1.87	111	102	9
E. coli (Dead)		91	72	26

While DEP was considered to be the major phenomenon that caused the trapping of live and dead cells at distinct locations (**Fig. 3a**) in the 2004 study,[11] the recent reports on EP_{NL} illustrate that this was not the case. A set of COMSOL simulations using the voltage employed in the separation in **Figure 3e**, and the conditions/parameters in **Table S8**, were conducted to further explore the individual contributions of each one the four EK phenomena considered in this study: EOF, EP_L, EP_{NL} and DEP. **Table 4** shows the overall velocity and average velocity values for each EK phenomena estimated across the cutline described in **Figure S2**. The data from the COMSOL simulations clearly illustrate that the magnitude of the DEP velocity is at least four orders of magnitude lower than the contributions of the other three EK phenomena. To further illustrate this, a plot depicting the velocity contributions of each phenomenon across the cutline defined in **Figure S2** is included as **Figure S4** where it is clearly observed that DEP has a negligible contribution.

Table 4. Individual contributions of each one of the four EK phenomena towards the overall velocity of the cells.

	$\mathbf{v}_{EO}$ (m/s)	Live *E. coli* cells				Dead *E. coli* cells			
		$\mathbf{v}_P$ (m/s)	$\mathbf{v}_{EP,L}$ (m/s)	$\mathbf{v}_{EP,NL}^{(3)}$ (m/s)	$\mathbf{v}_{DEP}$ (m/s)	$\mathbf{v}_P$ (m/s)	$\mathbf{v}_{EP,L}$ (m/s)	$\mathbf{v}_{EP,NL}^{(3)}$ (m/s)	$\mathbf{v}_{DEP}$ (m/s)
Current Study	6.3×10^{-4}	3.2×10^{-4}	-2.7×10^{-4}	-4.2×10^{-5}	3.8×10^{-9}	4.0×10^{-4}	-1.9×10^{-4}	-3.2×10^{-5}	-3.5×10^{-9}
2004 Study[11]	4.6×10^{-3}	-5.4×10^{-3}	-1.9×10^{-3}	-8.1×10^{-3}	-5.4×10^{-8}	-3.0×10^{-3}	-1.4×10^{-3}	-6.2×10^{-3}	5.0×10^{-8}

As seen in **Table 4** and **Figure S5**, the contribution of DEP is minimal and negligible for live and dead cells, while DEP is present, it has a contribution to the overall cell velocity that is orders of magnitude lower than the other three EK phenomena, thus, DEP is not dominant nor significant in this system under the employed conditions. This also holds true in the 2004 report by Lapizco-Encinas *et al*.,[11] under an electric field of 600 V/cm where the DEP velocity contribution is five orders of magnitude lower than the other EK phenomena present in the system as also shown in **Table 4**. For the velocity estimations for the 2004 study,[11] a cutline of 250 µm was considered

(cutline shown in **Fig. S4**) and the values of EO and EP mobilities from the current work were utilized, as the 2004 study did not contain any mobility data (see **Table S8**). The COMSOL results in **Table 4** for the 2004 study, although not entirely accurate, allow comparing relative magnitudes of the four EK phenomena. As an additional note, by employing more recently reported values of the conductivity of cell membranes (**Table 1**),[53,54] the value of the f_{CM} of the dead cells is actually positive ($f_{CM,\ Dead} = 0.38$), which means that dead *E. coli* cells should exhibit pDEP behavior.

CONCLUSIONS

This study is the first report of an electrophoretic-based separation of a binary mixture of live and dead *E. coli* cells in an iEK microfluidic device employing DC potentials. Two decades ago, the discrimination between live and dead *E. coli* cells in an iEK channel had been reported, but the distinction between the two cells types was attributed to dielectrophoretic effects.[11] The present report illustrated that DEP effects are minimal and that effective discrimination between live and dead cells is achieved by electrophoretic effects, with contributions from linear and nonlinear electrophoresis. After the characterization of the electrophoretic mobilities of the cells and COMSOL simulations to identify appropriate DC voltages for a successful separation, a set of separation experiments was performed achieving a separation resolution (Rs) of 1.87. Experimental repetitions had good reproducibility (deviations < 11 %) and good agreement with modeling results (deviations < 26 %) in terms of retention times. The findings from this study are twofold: First, an updated analysis was presented for the results reported in 2004 on the differential trapping of live and dead *E. coli* cells.[11] Second, an electrophoretic approach to live and dead cells separations was successfully demonstrated in a T-cross iEK microchannel under DC potentials. Further, the proposed electrophoretic approach only requires 3 minutes for a complete elution of live and dead cells as separate peaks in an electropherogram, opening the potential for iEK systems as platforms for rapid cell viability assessments.

ASSOCIATED CONTENT

Supporting Information

The supplementary file contains **Tables S1-S8** and **Figures S1-S4**. Additionally, the video file **Video_S1.mp4** showing the separation is also included. The video depicts simultaneously the elution of the *E. coli* cells and the acquisition of the fluorescence as a function of time.

Author Information

Corresponding Author

Blanca H. Lapizco-Encinas − Microscale Bioseparations Laboratory and Biomedical Engineering Department, Rochester Institute of Technology, Rochester, New York 14623, United States; orcid.org/0000-0001-6283-8210; Email: bhlbme@rit.edu

Authors

Viswateja Kasarabada - Microscale Bioseparations Laboratory and Biomedical Engineering Department, Rochester Institute of Technology, Rochester, New York 14623, United States; orcid.org/0000-0003-3238-3168.

Nuzhet Nihaar Nasir Ahamed - Microscale Bioseparations Laboratory and Biomedical Engineering Department,

Rochester Institute of Technology, Rochester, New York 14623, United States; orcid.org/0000-0002-2466-6216.

Alaleh Vaghef-Koodehi - Microscale Bioseparations Laboratory and Biomedical Engineering Department, Rochester Institute of Technology, Rochester, New York 14623, United States; orcid.org/0000-0001-7829-3374.

Gabriela Martinez-Martinez - Microscale Bioseparations Laboratory and Biomedical Engineering Department, Rochester Institute of Technology, Rochester, New York 14623, United States; orcid.org/0009-0007-8888-1170.

Author contributions

VK: Experimentation, data analysis, writing original draft – review & editing. **NNNA:** Experimentation, writing original draft – review & editing. **AVK:** Data Analysis, Writing Original Draft – Review & Editing. **GMM:** Data Analysis, Writing Original Draft – Review & Editing. **BHLE:** Conceptualization, methodology, project administration, supervision, writing original draft – review & editing.

Notes:

The authors declare no competing financial interest.

ACKNOWLEDGMENTS

This material is based upon work supported by the National Science Foundation under Award No. 2127592. The authors acknowledge Research Computing at the Rochester Institute of Technology for providing computational resources and support that have contributed to the research results reported in this publication.

REFERENCES

(1) Alali, S. A.; Shrestha, E.; Kansakar, A. R.; Parekh, A.; Dadkhah, S.; Peacock, W. F. Community Hospital Stethoscope Cleaning Practices and Contamination Rates. *Am. J. Infect. Control* **2020**, *48* (11), 1365–1369. https://doi.org/10.1016/j.ajic.2020.04.019.

(2) William A. Rutala, Ph.D., M. P. . Guideline for Disinfection and Sterilization in Healthcare Facilities: Updated 2017. *Healthcare Infection Control Practices Advisory Committee*. 2017, pp 1–158.

(3) Moore, J. H.; Honrado, C.; Stagnaro, V.; Kolling, G.; Warren, C. A.; Swami, N. S. Rapid in Vitro Assessment of Clostridioides Difficile Inhibition by Probiotics Using Dielectrophoresis to Quantify Cell Structure Alterations. *ACS Infect. Dis.* **2020**, *6* (5), 1000–1007. https://doi.org/10.1021/acsinfecdis.9b00415.

(4) Huang, D.; Man, J.; Jiang, D.; Zhao, J.; Xiang, N. Inertial Microfluidics: Recent Advances. *Electrophoresis* **2020**, *41* (24), 2166–2187. https://doi.org/10.1002/ELPS.202000134.

(5) Vaghef-Koodehi, A.; Lapizco-Encinas, B. H. Microscale Electrokinetic-Based Analysis of Intact Cells and Viruses. *Electrophoresis* **2022**, *43* (1–2), 263–287. https://doi.org/10.1002/elps.202100254.

(6) Xuan, X. Recent Advances in Direct Current Electrokinetic Manipulation of Particles for Microfluidic Applications. *Electrophoresis*. John Wiley & Sons, Ltd September 1, 2019, pp 2484–2513. https://doi.org/10.1002/elps.201900048.

(7) Song, Y.; Li, D.; Xuan, X. Recent Advances in Multimode Microfluidic Separation of Particles and Cells. *Electrophoresis*. John Wiley & Sons, Ltd June 1, 2023, pp 910–937. https://doi.org/10.1002/elps.202300027.

(8) Lapizco-Encinas, B. H. Nonlinear Electrokinetic Methods of Particles and Cells. *Annu. Rev. Anal. Chem.* **2024**, *17* (1), 243–264. https://doi.org/10.1146/annurev-anchem-061622-040810.

(9) Patel, P.; Markx, G. H. Dielectric Measurement of Cell Death. *Enzyme Microb. Technol.* **2008**, *43* (7), 463–470. https://doi.org/10.1016/j.enzmictec.2008.09.005.

(10) Pohl, H. A.; Hawk, I. Separation of Living and Dead Cells by Dielectrophoresis. *Science (80-.).* **1966**, *152* (3722), 647–649. https://doi.org/10.1126/science.152.3722.647-a.

(11) Lapizco-Encinas, B. H.; Simmons, B. A.; Cummings, E. B.; Fintschenko, Y. Dielectrophoretic

Concentration and Separation of Live and Dead Bacteria in an Array of Insulators. *Anal. Chem.* **2004**, *76* (6), 1571–1579. https://doi.org/10.1021/ac034804j.
(12) Fernandez, R. E.; Rohani, A.; Farmehini, V.; Swami, N. S. Review: Microbial Analysis in Dielectrophoretic Microfluidic Systems. *Anal. Chim. Acta* **2017**, *966*, 11–33. https://doi.org/10.1016/j.aca.2017.02.024.
(13) Hakim, K. S.; Lapizco-Encinas, B. H. Analysis of Microorganisms with Nonlinear Electrokinetic Microsystems. *Electrophoresis* **2021**, *42* (5), 588–604. https://doi.org/10.1002/elps.202000233.
(14) Li, H.; Bashir, R. Dielectrophoretic Separation and Manipulation of Live and Heat-Treated Cells of Listeria on Microfabricated Devices with Interdigitated Electrodes. *Sensors Actuators, B Chem.* **2002**, *86* (2–3), 215–221. https://doi.org/10.1016/S0925-4005(02)00172-7.
(15) Jen, C.-P.; Chen, T.-W. Selective Trapping of Live and Dead Mammalian Cells Using Insulator-Based Dielectrophoresis within Open-Top Microstructures. *Biomed. Microdevices* **2009**, *11* (3), 597–607.
(16) Iliescu, C.; Tresset, G.; Iliescu, F. S.; Sterian, P. E. Live/Dead Cell Assay Based on Dielectrophoresis-on-a-Chip. *UPB Sci. Bull. Ser. A Appl. Math. Phys.* **2010**, *72* (1), 33–44.
(17) Patel, S.; Showers, D.; Vedantam, P.; Tzeng, T. R.; Qian, S.; Xuan, X. Microfluidic Separation of Live and Dead Yeast Cells Using Reservoir-Based Dielectrophoresis. *Biomicrofluidics* **2012**, *6* (3), 34102–34112. https://doi.org/10.1063/1.4732800.
(18) Shafiee, H.; Sano, M. B.; Henslee, E. A.; Caldwell, J. L.; Davalos, R. V. Selective Isolation of Live/Dead Cells Using Contactless Dielectrophoresis (CDEP). *Lab Chip* **2010**, *10* (4), 438–445. https://doi.org/10.1039/b920590j.
(19) Zellner, P.; Shake, T.; Hosseini, Y.; Nakidde, D.; Riquelme, M. V.; Sahari, A.; Pruden, A.; Behkam, B.; Agah, M. 3D Insulator-Based Dielectrophoresis Using DC-Biased, AC Electric Fields for Selective Bacterial Trapping. *Electrophoresis* **2015**, *36* (2), 277–283. https://doi.org/10.1002/elps.201400236.
(20) Ettehad, H. M.; Wenger, C. Characterization and Separation of Live and Dead Yeast Cells Using Cmos-Based Dep Microfluidics. *Micromachines* **2021**, *12* (3), 270. https://doi.org/10.3390/mi12030270.
(21) Ettehad, H. M.; Zarrin, P. S.; Hölzel, R.; Wenger, C. Dielectrophoretic Immobilization of Yeast Cells Using CMOS Integrated Microfluidics. *Micromachines* **2020**, *11* (5), 501. https://doi.org/10.3390/MI11050501.
(22) Pudasaini, S.; Perera, A. T. K.; Das, D.; Ng, S. H.; Yang, C. Continuous Flow Microfluidic Cell Inactivation with the Use of Insulating Micropillars for Multiple Electroporation Zones. *Electrophoresis* **2019**, *40* (18–19), 2522–2529. https://doi.org/10.1002/elps.201900150.
(23) Pudasaini, S.; Perera, A. T. K.; Ng, S. H.; Yang, C. Bacterial Inactivation via Microfluidic Electroporation Device with Insulating Micropillars. *Electrophoresis* **2021**, *42* (9–10), 1093–1101. https://doi.org/10.1002/elps.202000326.
(24) Pudasaini, S.; Perera, A. T. K.; Ahmed, S. S. U.; Chong, Y. B.; Ng, S. H.; Yang, C. An Electroporation Device with Microbead-Enhanced Electric Field for Bacterial Inactivation. *Inventions* **2020**, *5* (1), 2. https://doi.org/10.3390/inventions5010002.
(25) Ho, B. D.; Beech, J. P.; Tegenfeldt, J. O. Cell Sorting Using Electrokinetic Deterministic Lateral Displacement. *Micromachines* **2021**, *12* (1), 1–14. https://doi.org/10.3390/mi12010030.
(26) Rouhi Youssefi, M.; Diez, F. J. Ultrafast Electrokinetics. *Electrophoresis* **2016**, *37* (5–6), 692–698. https://doi.org/10.1002/elps.201500392.
(27) Tottori, S.; Misiunas, K.; Keyser, U. F.; Bonthuis, D. J. Nonlinear Electrophoresis of Highly Charged Nonpolarizable Particles. *Phys. Rev. Lett.* **2019**, *123* (1), 14502. https://doi.org/10.1103/PhysRevLett.123.014502.
(28) Cardenas-Benitez, B.; Jind, B.; Gallo-Villanueva, R. C.; Martinez-Chapa, S. O.; Lapizco-Encinas, B. H.; Perez-Gonzalez, V. H. Direct Current Electrokinetic Particle Trapping in Insulator-Based Microfluidics: Theory and Experiments. *Anal. Chem.* **2020**, *92* (19), 12871–12879. https://doi.org/10.1021/acs.analchem.0c01303.
(29) Vaghef-koodehi, A.; Ernst, O. D.; Lapizco-Encinas, B. H. Separation of Cells and Microparticles in Insulator-Based Electrokinetic Systems. *Anal. Chem.* **2023**, *95* (2), 1409–1418. https://doi.org/10.1021/acs.analchem.2c04366.
(30) Nasir Ahamed, N. N.; Mendiola-Escobedo, C. A.; Perez-Gonzalez, V. H.; Lapizco-Encinas, B. H. Assessing the Discriminatory Capabilities of IEK Devices under DC and DC-Biased AC Stimulation Potentials.

Micromachines **2023**, *14* (12). https://doi.org/10.3390/mi14122239.
(31) Antunez-Vela, S.; Perez-Gonzalez, V. H.; Coll De Peña, A.; Lentz, C. J.; Lapizco-Encinas, B. H. Simultaneous Determination of Linear and Nonlinear Electrophoretic Mobilities of Cells and Microparticles. *Anal. Chem.* **2020**, *92* (22), 14885–14891. https://doi.org/10.1021/acs.analchem.0c03525.
(32) Dukhin, A. S.; Dukhin, S. S. Aperiodic Capillary Electrophoresis Method Using an Alternating Current Electric Field for Separation of Macromolecules. *Electrophoresis* **2005**, *26* (11), 2149–2153. https://doi.org/10.1002/elps.200410408.
(33) Dukhin, S. S. Electrokinetic Phenomena of the Second Kind and Their Applications. *Adv. Colloid Interface Sci.* **1991**, *35* (C), 173–196. https://doi.org/10.1016/0001-8686(91)80022-C.
(34) Dukhin, S. S. Electrophoresis at Large Peclet Numbers. *Adv. Colloid Interface Sci.* **1991**, *36* (C), 219–248. https://doi.org/10.1016/0001-8686(91)80034-H.
(35) Mishchuk, N. A.; Barinova, N. O. Theoretical and Experimental Study of Nonlinear Electrophoresis. *Colloid J.* **2011**, *73* (1), 88–96. https://doi.org/10.1134/S1061933X11010133.
(36) Ernst, O. D.; Vaghef-Koodehi, A.; Dillis, C.; Lomeli-Martin, A.; Lapizco-Encinas, B. H. Dependence of Nonlinear Electrophoresis on Particle Size and Electrical Charge. *Anal. Chem.* **2023**, *95* (16), 6595–6602. https://doi.org/10.1021/acs.analchem.2c05595.
(37) Lomeli-Martin, A.; Ernst, O. D.; Cardenas-Benitez, B.; Cobos, R.; Khair, A. S.; Lapizco-Encinas, B. H. Characterization of the Nonlinear Electrophoretic Behavior of Colloidal Particles in a Microfluidic Channel. *Anal. Chem.* **2023**, *95* (16), 6740–6747. https://doi.org/10.1021/acs.analchem.3c00782.
(38) Bentor, J.; Dort, H.; Chitrao, R. A.; Zhang, Y.; Xuan, X. Nonlinear Electrophoresis of Dielectric Particles in Newtonian Fluids. *Electrophoresis* **2023**, *44* (11–12), 938–946. https://doi.org/10.1002/elps.202200213.
(39) Bentor, J.; Xuan, X. Nonlinear Electrophoresis of Nonspherical Particles in a Rectangular Microchannel. *Electrophoresis* **2023**. https://doi.org/10.1002/ELPS.202300188.
(40) Vaghef-Koodehi, A.; Dillis, C.; Lapizco-Encinas, B. H. High-Resolution Charge-Based Electrokinetic Separation of Almost Identical Microparticles. *Anal. Chem.* **2022**, *94* (17), 6451–6456. https://doi.org/10.1021/acs.analchem.2c00355.
(41) Nasir Ahamed, N. N.; Mendiola-Escobedo, C. A.; Ernst, O. D.; Perez-Gonzalez, V. H.; Lapizco-Encinas, B. H. Fine-Tuning the Characteristic of the Applied Potential To Improve AC-IEK Separations of Microparticles. *Anal. Chem.* **2023**, *95* (26), 9914–9923. https://doi.org/10.1021/ACS.ANALCHEM.3C00995.
(42) Dutta, P.; Beskok, A. Analytical Solution of Combined Electroosmotic/Pressure Driven Flows in Two-Dimensional Straight Channels: Finite Debye Layer Effects. *Anal. Chem.* **2001**, *73* (9), 1979–1986. https://doi.org/10.1021/ac001182i.
(43) Klaseboer, E.; Chan, D. Y. C. On the Derivation of the Smoluchowski Result of Electrophoretic Mobility. *J. Colloid Interface Sci.* **2020**, *568*, 176–184. https://doi.org/10.1016/J.JCIS.2020.02.032.
(44) Jayaraman, A. S.; Klaseboer, E.; Chan, D. Y. C. The Unusual Fluid Dynamics of Particle Electrophoresis. *J. Colloid Interface Sci.* **2019**, *553*, 845–863. https://doi.org/10.1016/J.JCIS.2019.06.029.
(45) Schnitzer, O.; Yariv, E. Nonlinear Electrophoresis at Arbitrary Field Strengths: Small-Dukhin-Number Analysis. *Phys. Fluids* **2014**, *26* (12), 122002. https://doi.org/10.1063/1.4902331.
(46) Coll De Peña, A.; Miller, A.; Lentz, C. J.; Hill, N.; Parthasarathy, A.; Hudson, A. O.; Lapizco-Encinas, B. H. Creation of an Electrokinetic Characterization Library for the Detection and Identification of Biological Cells. *Anal. Bioanal. Chem.* **2020**, *412* (16), 3935–3945. https://doi.org/10.1007/s00216-020-02621-9.
(47) Duffy, D. C.; McDonald, J. C.; Schueller, O. J. A.; Whitesides, G. M. Rapid Prototyping of Microfluidic Systems in Poly(Dimethylsiloxane). *Anal. Chem.* **1998**, *70* (23), 4974–4984. https://doi.org/10.1021/ac980656z.
(48) Saucedo-Espinosa, M. A.; Lapizco-Encinas, B. H. Refinement of Current Monitoring Methodology for Electroosmotic Flow Assessment under Low Ionic Strength Conditions. *Biomicrofluidics* **2016**, *10* (3), 033104. https://doi.org/10.1063/1.4953183.
(49) Brown, D. Spectroscopy Using the Tracker Video Analysis Program. **2004**.
(50) Song, C.; Tao, Y.; Liu, W.; Chen, Y.; Yang, R.; Guo, W.; Li, B.; Ren, Y. Electrokinetic Behavior of an Individual Liquid Metal Droplet in a Rotating Electric Field. *Phys. Fluids* **2024**, *36* (1).

https://doi.org/10.1063/5.0184230/2932901.
(51) Vaghef-Koodehi, A.; Cyr, P.; Lapizco-Encinas, B. H. Improving Device Design in Insulator-Based Electrokinetic Tertiary Separations. *J. Chromatogr. A* **2024**, *1722*, 464853. https://doi.org/10.1016/j.chroma.2024.464853.
(52) Kłodzińska, E.; Szumski, M.; Dziubakiewicz, E.; Hrynkiewicz, K.; Skwarek, E.; Janusz, W.; Buszewski, B. Effect of Zeta Potential Value on Bacterial Behavior during Electrophoretic Separation. *Electrophoresis* **2010**, *31* (9), 1590–1596. https://doi.org/10.1002/elps.200900559.
(53) Castellarnau, M.; Errachid, A.; Madrid, C.; Juárez, A.; Samitier, J.; Juarez, A.; Samitier, J. Dielectrophoresis as a Tool to Characterize and Differentiate Isogenic Mutants of Escherichia Coli. *Biophys. J.* **2006**, *91* (10), 3937–3945. https://doi.org/10.1529/biophysj.106.088534.
(54) Pethig, R.; Markx, G. H. Applications of Dielectrophoresis in Biotechnology. *Trends Biotechnol.* **1997**, *15* (10), 426–432.
(55) Moncada-Hernández, H.; Lapizco-Encinas, B. H. Simultaneous Concentration and Separation of Microorganisms: Insulator-Based Dielectrophoretic Approach. *Anal. Bioanal. Chem.* **2010**, *396* (5), 1805–1816. https://doi.org/10.1007/s00216-009-3422-4.
(56) Lapizco-Encinas, B. H. Microscale Electrokinetic Assessments of Proteins Employing Insulating Structures. *Curr. Opin. Chem. Eng.* **2020**, *29*, 9–16. https://doi.org/10.1016/J.COCHE.2020.02.007.
(57) Markx, G. H.; Rousselet, J.; Pethig, R. DEP-FFF: Field-Flow Fractionation Using Non-Uniform Electric Fields. *J. Liq. Chromatogr. Relat. Technol.* **1997**, *20* (16–17), 2857–2872.
(58) Gallo-Villanueva, R. C.; Jesús-Pérez, N. M.; Martínez-López, J. I.; Pacheco, A.; Lapizco-Encinas, B. H. Assessment of Microalgae Viability Employing Insulator-Based Dielectrophoresis. *Microfluid. Nanofluidics* **2011**, *10* (6), 1305–1315.

For Table of Contents Only